Cholesterol pathway inhibition induces TGFβ signaling to promote basal differentiation in pancreatic cancer

Linara Gabitova-Cornell, *et al*., Igor Astsaturov

SUPPLEMENTARY FIGURES AND LIST OF SUPPLEMENTARY TABLES

SUPPLEMENTARY FIGURES

Figure S1

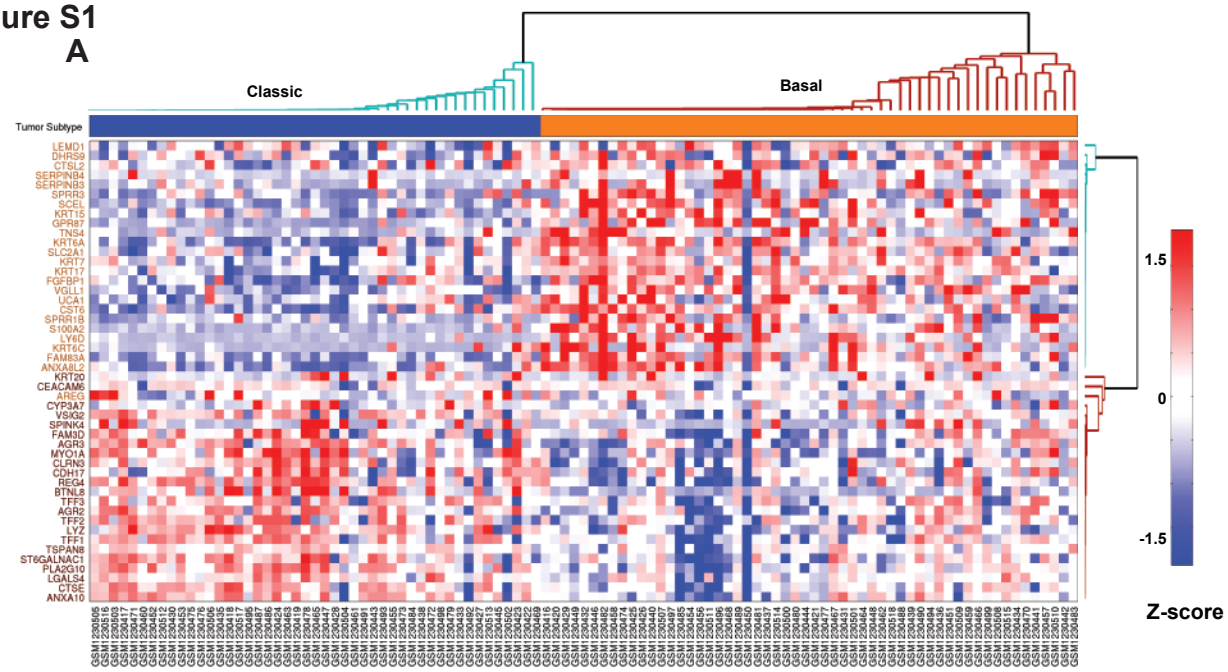

Figure S1. Analysis of mRNA signatures of pancreatic adenocarcinoma reported by the International Cancer Genome Consortium (ICGC, GSE50827). Related to figure 1.

(**A**) Heat map of unsupervised clustering analysis of 103 PDAC cases from ICGC based of gene expression signatures segregating classic or basal subsets by a weighted gene expression algorithm (Moffitt et al., 2015). Z-scores calculated for each gene are plotted on a red (higher expression) and blue (low expression) scale.

(**B**) Comparison of Reactome “cholesterol biosynthesis” signature genes expression in basal and classic PDAC cases from ICGC (n=103).

(**C**) Kaplan-Meyer survival of 102 PDAC cases from ICGC dataset stratified by *Reactome_cholesterol_biosynthesis* gene signature and Moffitt basal or classic subset assignment. One case was excluded due to early death after surgery.

Figure S2

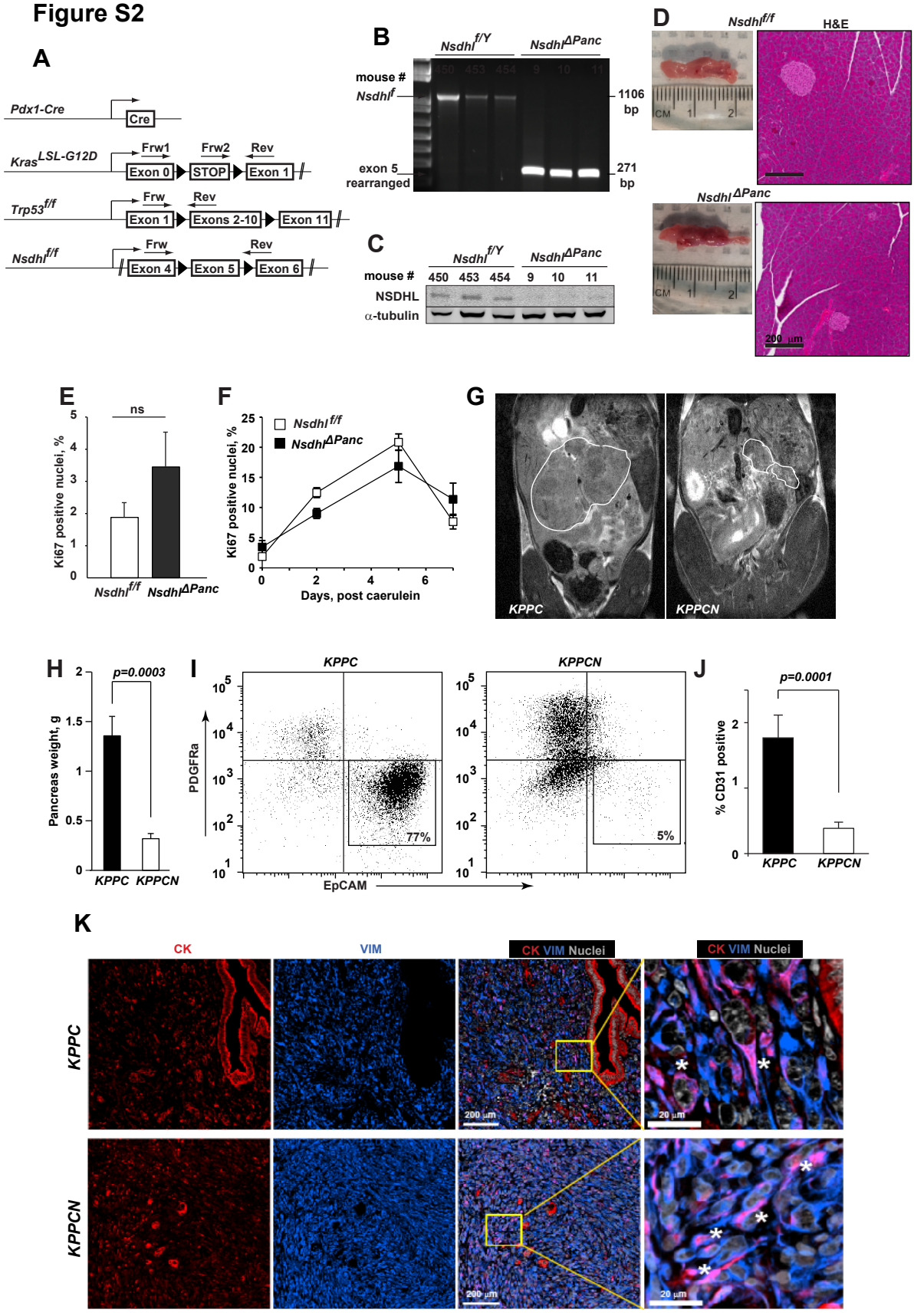
A
Pdx1-Cre
Cre
Kras LSL-G12D
Frw1
Frw2
Rev
Exon 0
STOP
Exon 1
Trp53 f/f
Frw
Rev
Exon 1
Exons 2-10
Exon 11
Nsdhl f/f
Frw
Rev
Exon 4
Exon 5
Exon 6
B
Nsdhl f/Y
Nsdhl ΔPanc
mouse #
Nsdhl f
450 453 454 9 10 11
1106 bp
exon 5 rearranged
271 bp
C
Nsdhl f/Y
Nsdhl ΔPanc
mouse # 450 453 454 9 10 11
NSDHL
α-tubulin
D
Nsdhl f/f
H&E
Nsdhl ΔPanc
200 µm
E
ns
Ki67 positive nuclei, %
Nsdhl f/f
Nsdhl ΔPanc
F
Nsdhl f/f
Nsdhl ΔPanc
Ki67 positive nuclei, %
Days, post caerulein
G
KPPC
KPPCN
H
p=0.0003
Pancreas weight, g
KPPC
KPPCN
I
KPPC
KPPCN
PDGFRa
EpCAM
77%
5%
J
p=0.0001
% CD31 positive
KPPC
KPPCN
K
CK
VIM
CK VIM Nuclei
CK VIM Nuclei
KPPC
KPPCN
200 µm
20 µm
200 µm
20 µm

Figure S2. Development of basal PDAC in mice with conditional knockout of *Nsdhl* in pancreatic epithelial cells. Related to figure 2.

A) Schema of KPC and KPCN genetic constructs. *Thick arrowheads*, *loxP* sites. *Frw* and *Rev*, location of genotyping primers (see STAR METHODS).

(**B**) Representative PCR products confirming rearrangement of $Nsdhl^{f}$ locus in males (*Nsdhl* is localized to the X-chromosome).

(**C**) Representative Western blot indicating loss of expression of NSDHL in pancreatic tissues of *Pdx1-Cre*-positive males. Similar findings were observed in homozygous $Nsdhl^{f/f}$ females (not shown).

(**D**) Representative images of $Nsdhl^{\Delta Panc}$ versus $Nsdhl^{f/f}$ pancreas.

(**E**) Quantification of Ki-67-positive nuclei as an indicator of proliferation in $Nsdhl^{\Delta Panc}$ versus $Nsdhl^{f/f}$ pancreatic tissues.

(**F**) Quantification of Ki-67-positive nuclei as an indicator of reparative proliferation following acute caerulein-induced pancreatic injury in pancreatic epithelial cells of $Nsdhl^{\Delta Panc}$ and $Nsdhl^{f/f}$ mice.

(**G**) Micro-MRI images of littermate mice of indicated genotypes, with outlined pancreatic tissues.

(**H**) Pancreas weights in *KPPC* and *KPPCN* mice at 7-8 weeks of age; *, p=0.0003.

(**I**) Expression of PDGFRα and EpCAM in representative *KPPC* and *KPPCN* tumors as determined by fluorescent activated cell sorting (FACS).

(**J**) Quantification of CD31 (PECAM) positive areas on tumor sections indicative of vascular endothelial cells; n=5 pancreatic tumors of each genotype.

(**K**) Representative images of multiplex immunofluorescence characterization of *KPPC* (top) and *KPPCN (bottom)* carcinoma, depicting cytokeratin (CK) positive cells in red, vimentin (Vim) positive cells in blue, and overlay for double-positive cells in purple. *Asterisks*, denote double-positive (CK+, VIM+) cells. In all graphs, error bars, SEM; indicated p-values by Wilcoxon test.

Table S3. Histological characterization of mouse adenocarcinoma. Related to Figure 2.

Sample#	PDAC histology	Age, days	Dominant PDAC component	PDAC grade	% high grade area
	Genotype ***KPC***, n=24				
13-5309	Early adenocarcinoma	129	glandular	1	0
13-5311	Differentiated adenocarcinoma	126	glandular	1	0
14-4602	Differentiated adenocarcinoma	142	glandular	1	0
14-4605	Poorly differentiated adenocarcinoma	197	solid	3	50
14-4612	Differentiated adenocarcinoma	154	glandular	1	10
14-4619	Moderately differentiated adenocarcinoma	122	glandular	2	0
14-4624	Moderately differentiated adenocarcinoma	153	glandular	2	20
15-0824	Moderately differentiated adenocarcinoma	170	glandular	2	10
15-0835	Differentiated adenocarcinoma	146	glandular	1	0
15-0847	Moderately differentiated adenocarcinoma	167	glandular	2	10
15-0848	Cystic adenocarcinoma	167	glandular	1	0
15-0859	Differentiated adenocarcinoma	101	glandular	1	0
15-0869	Small focus, moderately differentiated adenocarcinoma	90	glandular	2	10
15-0870	Differentiated adenocarcinoma	90	glandular	1	0
15-0871	Moderately differentiated adenocarcinoma with necrosis	136	glandular	2	10
16-1903	Small focus of moderately differentiated adenocarcinoma	141	glandular	2	0
16-1913	Poorly differentiated adenocarcinoma with necrosis	142	glandular	3	10
16-1917	Poorly differentiated adenocarcinoma	111	solid	3	50
16-1919	Poorly differentiated adenocarcinoma	111	glandular	3	50
16-1920	Small focus of differentiated adenocarcinoma	85	glandular	1	0
16-1925	Differentiated adenocarcinoma	112	glandular	1	0
16-1931	Moderately differentiated adenocarcinoma	111	glandular	2	10
16-1944	Small focus, adenocarcinoma	56	glandular	1	10
16-1958	Moderately differentiated adenocarcinoma	84	glandular	2	0
	Genotype ***KPCN***, n=3				
17-0188	Undifferentiated adenocarcinoma with sarcomatoid growth	122	solid	4	70
17-5817	Undifferentiated adenocarcinoma with sarcomatoid growth	170	solid	4	90
18-5102	Poorly differentiated adenocarcinoma	191	solid	3	<10%

Table S3 (*continued*). Histological characterization of mouse adenocarcinoma.

Sample ID	PDAC histology	Age, days	Dominant PDAC component	PDAC Grade	% high grade area
	Genotype ***KPPC***, n=15				
15-2865	Differentiated adenocarcinoma	54	glandular	1	10
15-2866	Differentiated adenocarcinoma	51	glandular	1	0
15-2867	Moderately differentiated adenocarcinoma	51	glandular	2	10
16-3827	Differentiated adenocarcinoma	63	glandular	1	20
16-3829	Moderately differentiated adenocarcinoma	63	glandular	2	10
17-0022	Differentiated adenocarcinoma	32	glandular	1	10
17-0197	Moderately differentiated adenocarcinoma	66	glandular	2	10
17-0198	Differentiated adenocarcinoma	70	glandular	1	<10
18-5014	Differentiated adenocarcinoma	64	glandular	1	<10
18-5015	Differentiated adenocarcinoma	64	glandular	1	0
18-5019	Poorly differentiated adenocarcinoma	51	glandular/solid	3	30
18-5020	Differentiated adenocarcinoma	66	glandular	1	0
18-5098	Differentiated adenocarcinoma	54	glandular	1	0
18-5099	Moderately differentiated adenocarcinoma	61	glandular	2	30
18-5100	Moderately differentiated adenocarcinoma	65	glandular	2	20
	Genotype ***KPPCN***, n=25				
16-3892	Microfocus of undifferentiated adenocarcinoma	56	solid	4	100
16-3910	Microfocus of undifferentiated adenocarcinoma	57	solid	4	100
16-3911	Microfocus of undifferentiated adenocarcinoma	57	solid	4	100
17-0020	Undifferentiated adenocarcinoma	82	solid	4	90
17-0036	Undifferentiated adenocarcinoma	94	solid	4	80
17-0179	Undifferentiated adenocarcinoma	86	solid	4	100
17-0183	Microfocus of undifferentiated adenocarcinoma	78	solid	4	100
17-0184	Differentiated adenocarcinoma	69	glandular	1	20
17-0185	Undifferentiated adenocarcinoma with sarcomatoid growth	84	solid	4	90
17-0186	Undifferentiated adenocarcinoma	75	solid	4	100
17-0189	Undifferentiated adenocarcinoma	80	solid	4	90
17-5809	Poorly differentiated adenocarcinoma	68	glandular	2	30
17-5814	Undifferentiated adenocarcinoma with sarcomatoid growth	78	solid	4	90
17-5815	Undifferentiated adenocarcinoma with	83	solid	4	100

	sarcomatoid growth				
17-5822	Differentiated adenocarcinoma	86	glandular	1	20
17-5823	Moderately differentiated adenocarcinoma	71	glandular	2	30
17-6714	Moderately differentiated adenocarcinoma	57	glandular	2	10
18-5016	Undifferentiated adenocarcinoma	75	solid	4	70
18-5088	Moderately differentiated adenocarcinoma	86	glandular	2	30
18-5091	Undifferentiated adenocarcinoma with sarcomatoid growth	71	solid	4	100
18-5092	Undifferentiated adenocarcinoma with sarcomatoid growth	88	solid	4	100
18-5093	Undifferentiated adenocarcinoma with sarcomatoid growth	88	solid	4	100
18-5094	Undifferentiated adenocarcinoma with sarcomatoid growth	87	solid	4	90
18-5095	Undifferentiated adenocarcinoma with sarcomatoid growth	70	solid	4	80
18-5097	Poorly differentiated adenocarcinoma	77	solid and glandular	3&4	50
	Genotype ***KPPC treated with Atorvastatin***, n=12				
19-2530	Adenocarcinoma	54	glandular	1	20
19-2533	Undifferentiated adenocarcinoma	61	solid	4	60
19-2534	Adenocarcinoma	70	glandular	1	10
19-2535	Undifferentiated adenocarcinoma with sarcomatoid growth	57	solid	4	70
19-2536	Undifferentiated adenocarcinoma with sarcomatoid growth	55	solid	3	40
19-2542	Adenocarcinoma	65	glandular	1	30
19-2543	Adenocarcinoma	65	glandular	2	30
19-2544	Adenocarcinoma	59	glandular	2	10
19-2545	Adenocarcinoma	64	glandular	1	20
19-2546	Undifferentiated adenocarcinoma with sarcomatoid growth	64	solid	4	60
19-2547	Adenocarcinoma	66	glandular	1	30
19-2548	Adenocarcinoma	66	glandular	2	40

Figure S3

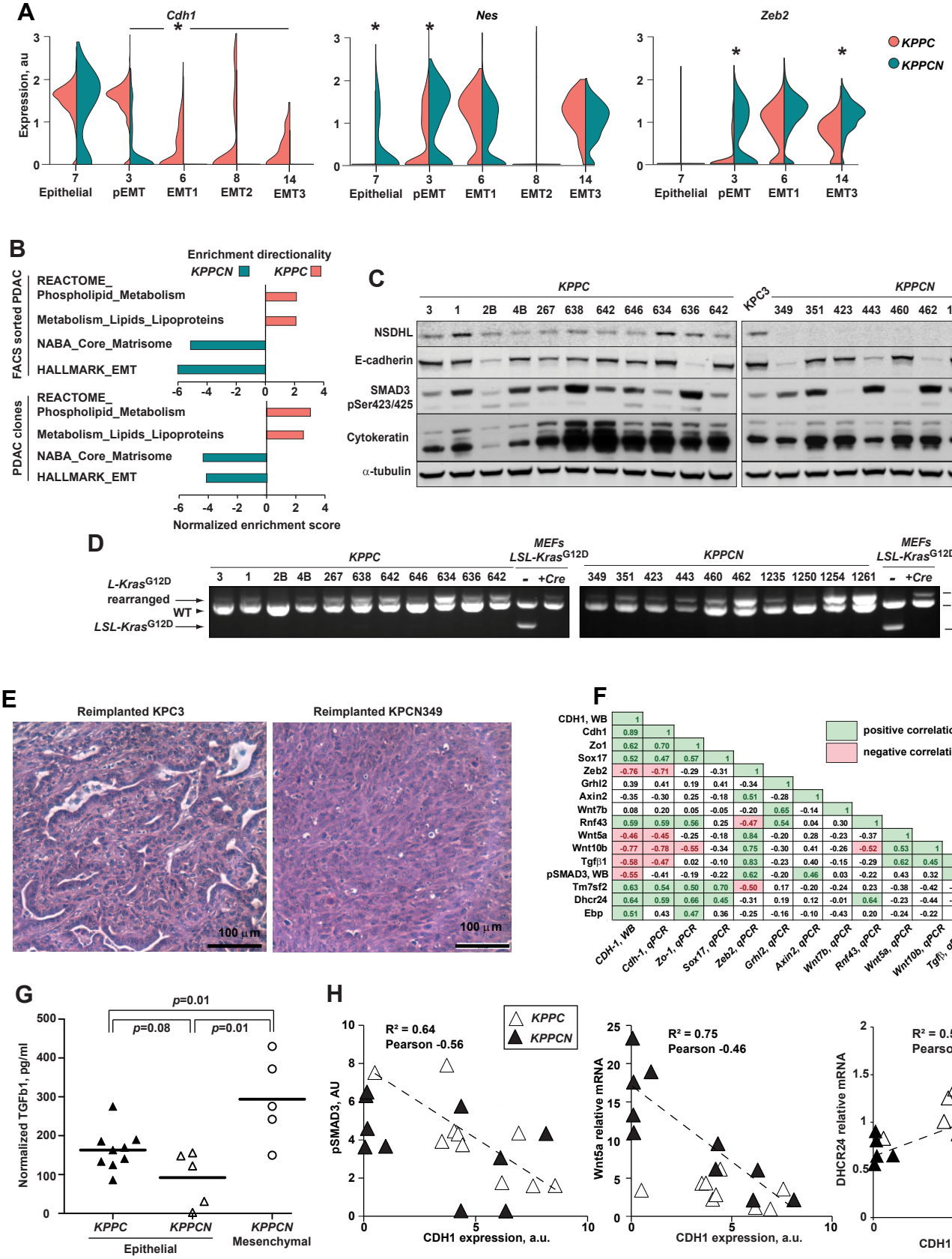
A
Cdh1
Nes
Zeb2
Expression, au
KPPC
KPPCN
7 Epithelial
3 pEMT
6 EMT1
8 EMT2
14 EMT3
B
Enrichment directionality
KPPCN
KPPC
FACS sorted PDAC
PDAC clones
REACTOME_ Phospholipid_Metabolism
Metabolism_Lipids_Lipoproteins
NABA_Core_Matrisome
HALLMARK_EMT
Normalized enrichment score
C
KPPC
KPPCN
KPC3
3 1 2B 4B 267 638 642 646 634 636 642
349 351 423 443 460 462 1235 1250 1254 1261
NSDHL
E-cadherin
SMAD3 pSer423/425
Cytokeratin
α-tubulin
D
KPPC
KPPCN
MEFs LSL-KrasG12D
L-KrasG12D rearranged
WT
LSL-KrasG12D
- +Cre
650bp
622bp
500bp
E
Reimplanted KPC3
Reimplanted KPCN349
100 μm
F
positive correlation, Pearson >0.45
negative correlation, Pearson <-0.45
CDH1, WB
Cdh1
Zo1
Sox17
Zeb2
Grhl2
Axin2
Wnt7b
Rnf43
Wnt5a
Wnt10b
Tgfβ1
pSMAD3, WB
Tm7sf2
Dhcr24
Ebp
G
p=0.01
p=0.08
p=0.01
Normalized TGFb1, pg/ml
KPPC
KPPCN
Epithelial
KPPCN
Mesenchymal
H
KPPC
KPPCN
R² = 0.64
Pearson -0.56
pSMAD3, AU
CDH1 expression, a.u.
R² = 0.75
Pearson -0.46
Wnt5a relative mRNA
CDH1 expression, a.u.
R² = 0.56
Pearson 0.64
DHCR24 relative mRNA
CDH1 expression, a.u.

Figure S3. ***Nsdhl*** **knockout promotes epithelial-to-mesenchymal transition. Related to figure 3.**

(**A**) Violin plot of normalized expression of *Cdh1, Nes* and Zeb2 in tumor cells corresponding to the indicated clusters; *, false discovery rate-adjusted $p<10^{-10}$ are shown for significant differences. *Y-axis*, normalized expression; *violin width*, cell density in each population.

(**B**) Normalized enrichment scores for FACS-sorted primary PDAC cells (n=3 of each genotype) and PDAC clones (n=3 of of each genotype). Shown are selected signatures with family-wise error rate, FWER<5%.

(**C**) Western blot of lysates from *KPPC* and *KPPCN* clones illustrating expression of pancreatic adenocarcinoma differentiation markers.

(**D**) PCR products confirming fully excised STOP sequence in *LSL-KRas^{G12D}* knock-in gene (bottom band ~500 bp) in indicated mouse PDAC cell lines.

(**E**) Representative hematoxylin-eosin images of pancreatic tumors arising from orthotopically implanted well-differentiated *KPPC* (KPC3) and basal *KPPCN* (KPCN349) pancretic carcinoma. Scale bars, 100 μm.

(**F**) Pearson correlation coefficients for multiple PDAC differentiation markers characterizing *KPPC* and *KPPCN* cell lines.

(**G**) Secreted TGFB1 in culture supernatants of KPPC and KPPCN cell lines; indicated *p*-values by Mann-Whitney test.

(**H**) Correlation of CDH1 expression with level of phosphorylated SMAD2/3, and mRNA for WNT5A and DHCR24, in *KPPC* and *KPPCN* clones; a.u., arbitrary units; R, correlation coefficient.

Figure S4

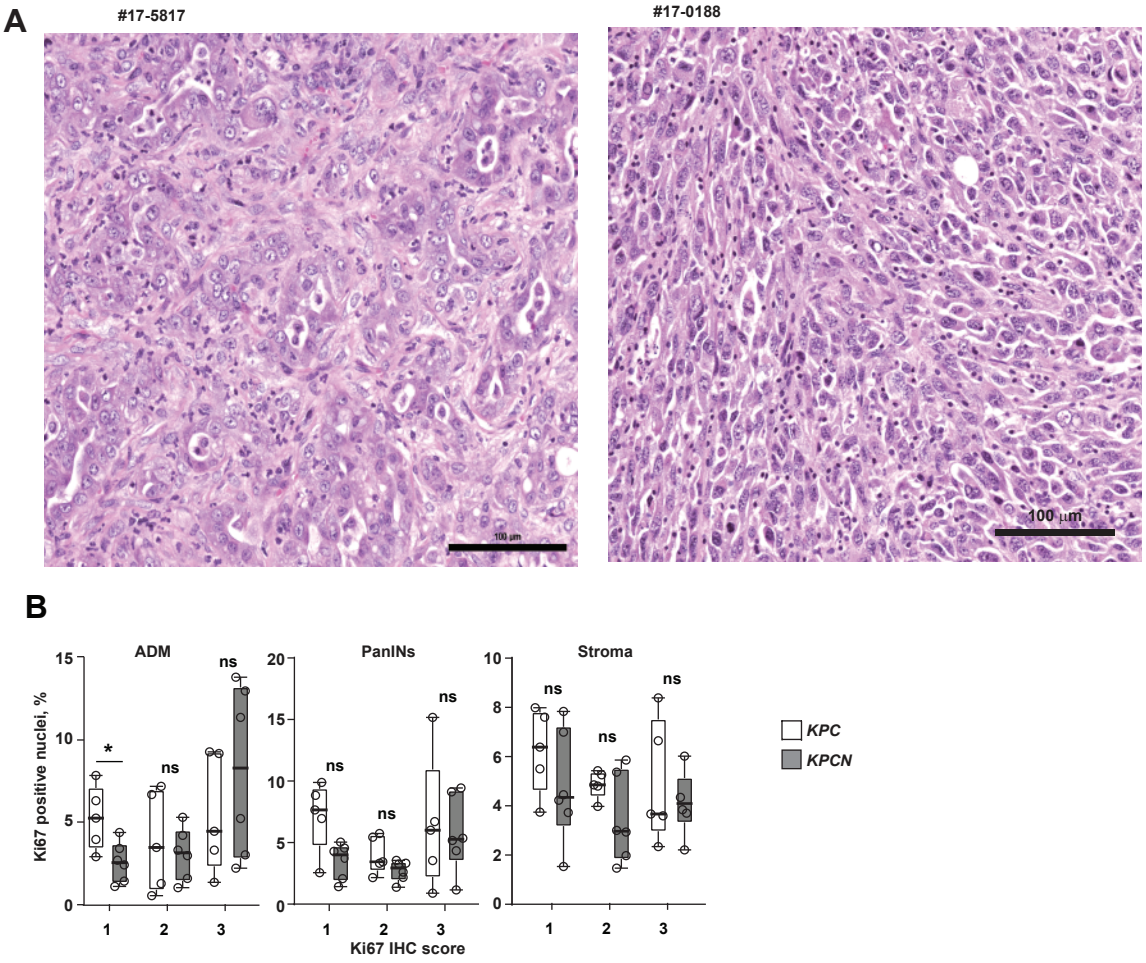
A
#17-5817
#17-0188
100 µm
B
ADM
PanINs
Stroma
Ki67 positive nuclei, %
Ki67 IHC score
ns
*
KPC
KPCN

Figure S4. **Pancreatic cancer prevention in *Nsdhl* conditional knockout depends on *Trp53*. Related to figure 4.**

(**A**) Hematoxylin and eosin images of grade 4 PDAC in two *KPCN* mice.

(**B**) Enumeration of Ki67-positive cells in pancreatic lesions and stromal cells in *KPC* and *KPCN* mice. *, $p<0.05$; ns, not significant, Wilcoxon test. Boxplots represent median (black bar) and full range of measurements.

Figure S5

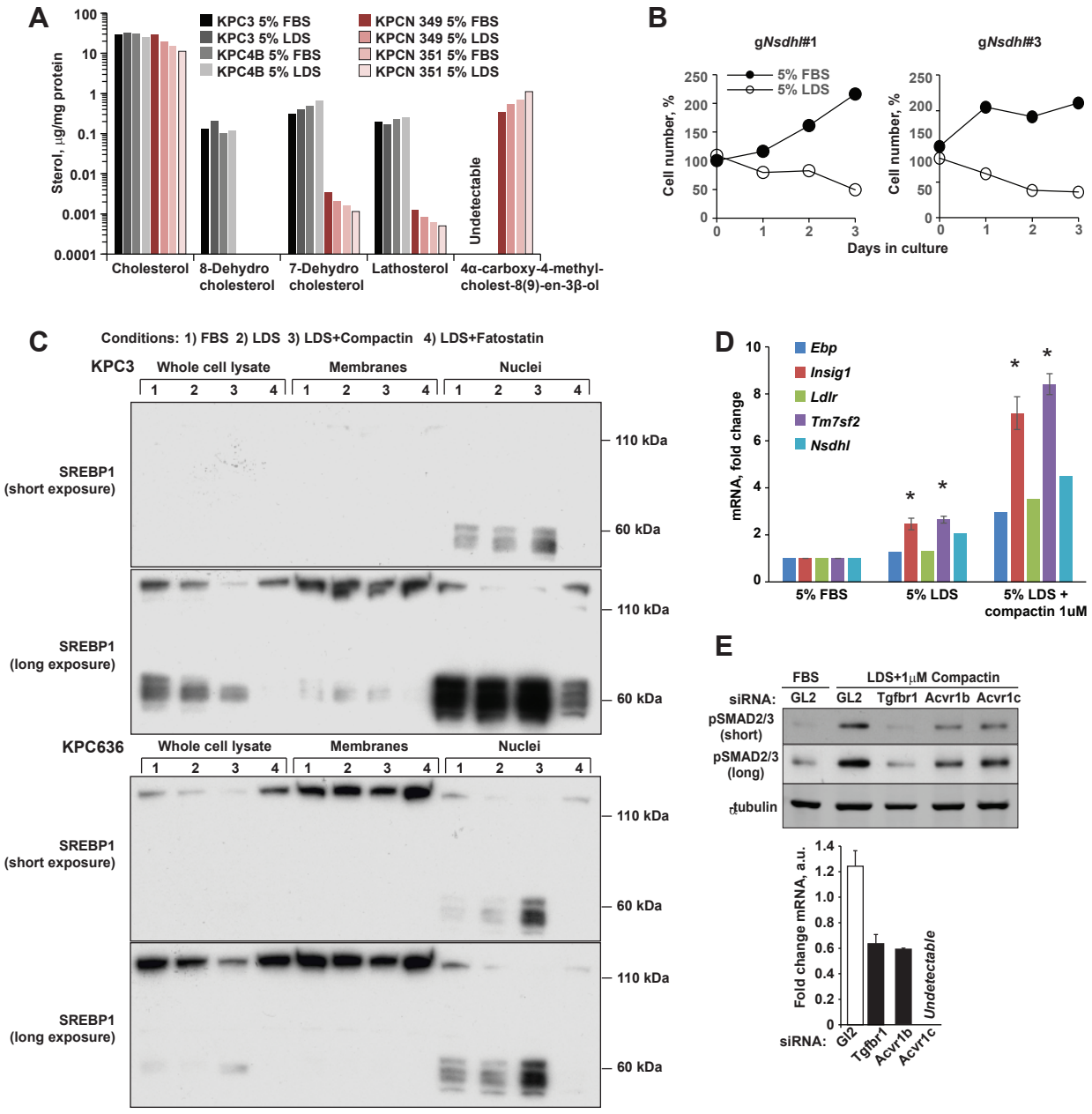
A
KPC3 5% FBS
KPC3 5% LDS
KPC4B 5% FBS
KPC4B 5% LDS
KPCN 349 5% FBS
KPCN 349 5% LDS
KPCN 351 5% FBS
KPCN 351 5% LDS
Sterol, μg/mg protein
Undetectable
Cholesterol
8-Dehydro cholesterol
7-Dehydro cholesterol
Lathosterol
4α-carboxy-4-methyl-cholest-8(9)-en-3β-ol
B
gNsdhl#1
gNsdhl#3
5% FBS
5% LDS
Cell number, %
Days in culture
C
Conditions: 1) FBS 2) LDS 3) LDS+Compactin 4) LDS+Fatostatin
KPC3
Whole cell lysate
Membranes
Nuclei
SREBP1 (short exposure)
SREBP1 (long exposure)
110 kDa
60 kDa
KPC636
D
Ebp
Insig1
Ldlr
Tm7sf2
Nsdhl
mRNA, fold change
5% FBS
5% LDS
5% LDS + compactin 1uM
E
FBS
LDS+1μM Compactin
siRNA:
GL2
Tgfbr1
Acvr1b
Acvr1c
pSMAD2/3 (short)
pSMAD2/3 (long)
α-tubulin
Fold change mRNA, a.u.
Undetectable

Figure S5. Cholesterol pathway perturbation activates SREBP1 and TGFβ pathway signaling in PDAC cells. Related to figure 5.

(**A**) Quantification of non-polar sterols by gas chromatography and mass spectrometry (GC-MS) in pancreatic carcinoma cell lines. Peak values were used to estimate sterol abundance, and results were normalized to total cellular protein content.

(**B**) Growth arrest of NSDHL-depleted KPC3 *Nsdhl*^{CRISPRi} PDAC cells as assessed by Alamar blue viability in 5% FBS and 5%LDS.

(**C**) Western blot showing full length (MW ~120 kDa) and activated ~68 kDa nuclear fragment of SREBP1 in fractionated cellular lysates of KPC3 (epithelial) and KPC636 (mesenchymal) PDAC cells grown for 48 hours with 5% FBS, 5% LDS+compactin, and 5% LDS+ 20 μM fatostatin.

(**D**) Quantitative RT-PCR determined expression of SREBP-regulated genes in KPC3 cells grown for 48 hours in DMEM supplemented with 5% FBS, 5% LDS, or 5% LDS with 1 μM compactin.

(**E**) Effects of *Tgfbr1*, *Acvr1b*, or *Acvr1c* siRNA knockdown on phosphorylated SMAD2/3 expression in KPC3 cells transfected with siRNA and conditioned for 48 hours in 5% FBS or in 5% LDS with 1 μM compactin. *Right,* RT-PCR validation of siRNA silencing of *Tgfbr1*, *Acvr1b* and *Acvr1c* in KPC3 PDAC cells.

Figure S6

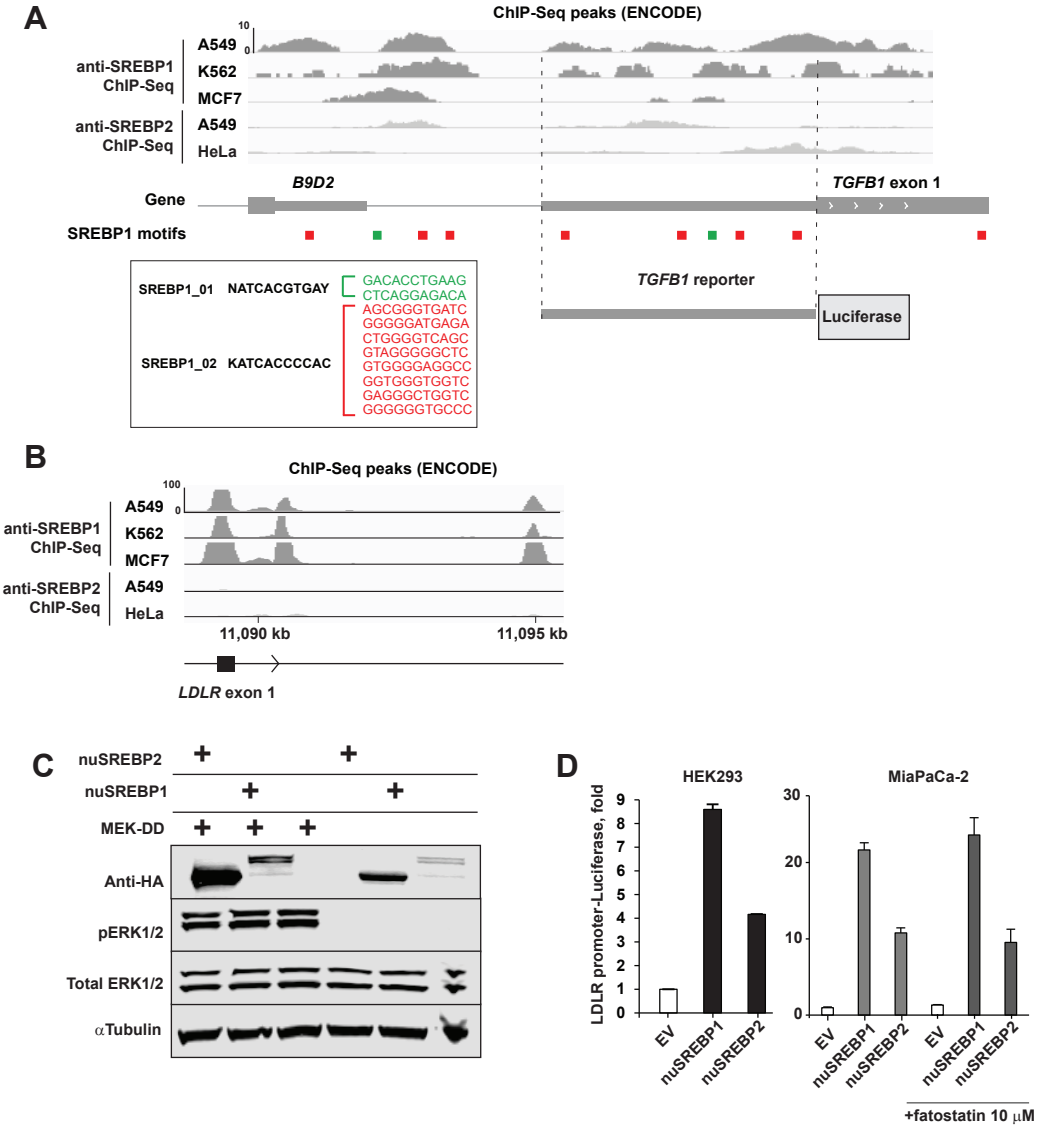
A
ChIP-Seq peaks (ENCODE)
anti-SREBP1 ChIP-Seq
anti-SREBP2 ChIP-Seq
A549
K562
MCF7
A549
HeLa
Gene
B9D2
TGFB1 exon 1
SREBP1 motifs
SREBP1_01 NATCACGTGAY
GACACCTGAAG
CTCAGGAGACA
SREBP1_02 KATCACCCCAC
AGCGGGTGATC
GGGGGATGAGA
CTGGGGTCAGC
GTAGGGGGCTC
GTGGGGAGGCC
GGTGGGTGGTC
GAGGGCTGGTC
GGGGGGTGCCC
TGFB1 reporter
Luciferase
B
ChIP-Seq peaks (ENCODE)
anti-SREBP1 ChIP-Seq
anti-SREBP2 ChIP-Seq
A549
K562
MCF7
A549
HeLa
11,090 kb
11,095 kb
LDLR exon 1
C
nuSREBP2
nuSREBP1
MEK-DD
Anti-HA
pERK1/2
Total ERK1/2
αTubulin
D
HEK293
MiaPaCa-2
LDLR promoter-Luciferase, fold
EV
nuSREBP1
nuSREBP2
+fatostatin 10 μM

Figure S6. Cholesterol depletion activates TGF pathway signaling via an autocrine mechanism. Related to figure 6.

(**A**) Presence of SREBP1 binding motifs (sequences shown in *box*) overlapping with chromatin immunoprecipitation and DNA sequencing (ChIP-Seq) peaks using anti-SREBP1 antibodies in human cancer cell lines (ENCODE.org). Binding peaks (relative scale 0-10) in the promoter region of human *TGFB1* gene are shown (gray), and consensus binding motifs for SREBP1 located within peaks are indicated, whereas no SREBP2 binding motifs and background level of SREBP2 binding was found by ChIP-seq.

(**B**) Comparison of binding peaks (relative scale 0-100) for SREBP1 and SREBP2 to LDLR promoter as determined by ChIP-Seq (ENCODE.org).

(**C**) Western blot of HA-tagged nuclear (nu) fragments of mouse SREBP1 (aa 1-480) and mouse SREBP2 (aa 1-473), following transfection of HEK293 cells with corresponding expression plasmids. Phosphorylated ERK1/2 reflects expression of constitutively active form of MEK1 (mutations S218D/S222D).

(**D**) Functional activity of nuSREBP1 and nuSREBP2 expression plasmid constructs in HEK293 cells by co-transfection with *LDLR*-luciferase reporter. Empty vector lacking SREBP served as a negative control for background activity of luciferase reporter. Fatostatin at 10 μM was used to block the endogenous SREBP activation. Data are represented as mean±SEM.

Figure S7

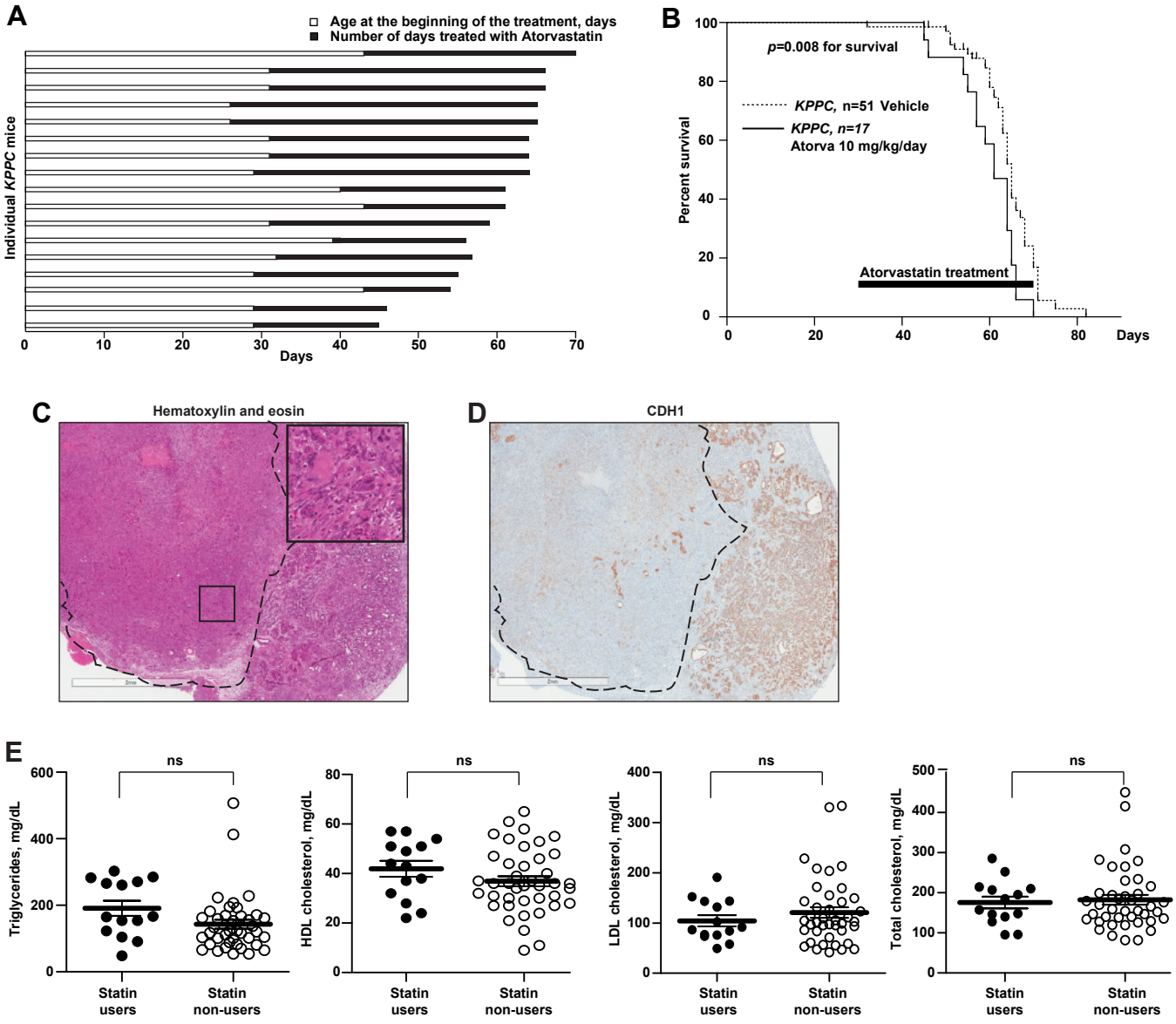
A
Age at the beginning of the treatment, days
Number of days treated with Atorvastatin
Individual KPPC mice
Days
B
p=0.008 for survival
KPPC, n=51 Vehicle
KPPC, n=17
Atora 10 mg/kg/day
Atorvastatin treatment
Percent survival
Days
C
Hematoxylin and eosin
D
CDH1
E
Triglycerides, mg/dL
HDL cholesterol, mg/dL
LDL cholesterol, mg/dL
Total cholesterol, mg/dL
ns
Statin users
Statin non-users

Figure S7. Cholesterol homeostasis perturbation with statins in *KPPC* mice and PDAC patients. Related to figure 7.

(**A**) Age at treatment onset and duration of atorvastatin treatment in a cohort of 17 KPPC mice. Each bar represents an individual animal. Pancreatic tissues were collected for histopathologic evaluation from all but 2 animals.

(**B**) Kaplan-Meyer survival probability of atorvastatin treated animals was compared to vehicle (water) *KPPC* control mice. A cohort of n=17, 4 week old *KPPC* mice received daily oral gavage of atorvastatin at 10 mg/kg/day until moribund. Survival of control animals (n=51) was estimated in the same colony with identical criteria for euthanasia in the setting of advanced pancreatic tumors.

(**C**) Hematoxylin and eosin and (**D**) E-cadherin (CDH1) staining of large focus of grade 4 basal PDAC marked by dashed line.

(**E**) Serum lipids levels in 55 PDAC patients separated by the statin usage status; Plots represent median (black bar) and range (25-75th percentile) of lipid level for individual cases shown as closed circles (statin users) and open circles (non-users); *ns*, not significant by two-way ANOVA test.

Supplementary Table 6. Primers for genotyping, CRISPRi and qPCR assays. Related to STAR Methods.

Primers for genotyping	**Sequence (5' to 3')**
Nsdhl exon5 rearrangement: Forward	gtg cta ctg tag act gaa cc
Nsdhl exon5 rearrangement: Reverse	gtg tcc ttg caa tct cag tg
Cre detection: oIMR1084 Forward	gcg gtc tgg cag taa aaa cta tc
Cre detection: oIMR1085 Reverse	gtg aaa cag cat tgc tgt cac tt
Internal control for Cre: oIMR7338 Forward	cta ggc cac aga att gaa aga tct
Internal control for Cre: oIMR7339 Reverse	gta ggt gga aat tct agc atc atc c
NSDHL flox5 detection: Forward	gtg cta ctg tag act gaa cc
NSDHL flox5 detection: Reverse	tct cct gga tgc tct gat ac
LSL-KRas detection and rearrangement: Forward 1	gtc ttt ccc cag cac agt gc
LSL-KRas detection and rearrangement: Forward 2	agc tag cca cca tgg ctt gag taa gtc tgc a
LSL-KRas detection and rearrangement: Reverse 1	ctc ttg cct acg cca cca gct c
Trp53 flox detection: oIMR8543 Forward	ggt taa acc cag ctt gac ca
Trp53 flox detection: oIMR8544 Reverse	gga ggc aga gac agt tgg ag
SYBR Green Assays	**Sequence (5' to 3')**
Grhl2	For CCCATGACCTACCTCAACAAA Rev CACCATCACCACACTCCTG
Wnt7b	For TCTCGTCGCTTTGTGGATG Rev CGGTCCTCCAGAACCTTTC
Wnt10b	For GAATGCGGATCCACAACAAC Rev CCCTCCAACAGGTCTTGAAT
Rnf43	For AAGGGAAGCTAATGCAGTCC Rev AGCTTGACGATGCTGATGAA
Sox17	For TTTATGGTGTGGGCCAAAGA Rev GCCTTCCAAGACTTGCCTAG
Axin2	For GTCTCTACCTCATTTTCCGAGAA Rev TCCAGCTCCAGTTTCAGTTT
Zo-1	For ACCATGCCTAAAGCTGTCCCT Rev TGTTAAAAATGCCACGAGCTGTAG
Tm7sf2	For GGCCTCATTGGCTGGGTT Rev AAGCCATTGACCAGCCACAT
Dhcr24	For GTGGAGAACTACCTGAAGACAAACC Rev CGAAAGGGATGATGTCCTGG
Ebp	For GTTTGCTGTGTGTACCTTCATTCA

	Rev ACGACGAAGCTGTCACTAAGGA
Tgfb2	For CTCAACACACCAAAGTCCTCA Rev TGTTCGATCTTGGGCGTATTT
Tgfb3	For CGCTACATAGGTGGCAAGAAT Rev AGACCCAAGTTGGACTCTCT
Insig1	For CTAGTGCTCTTCTCATTTGGCGT Rev GTAAACCGACAACAGCCGCT
Ldlr	For AGGCTGTGGGCTCCATAGG Rev TGCGGTCCAGGGTCATCT
Nsdhl	For GGAGCGAGGCTATACTGTCAATG Rev TTACACCTTTGAGAGCTGGGTACA
Pai1	For GTCTTCCTCCACAGCCTTT Rev CCATGAAGAGGATTGTCTCTGTC
Zeb1	For CCAAACGGAAACCAGGATGA Rev GGTCACATGCATACATTCCATTC
Acvr1b	For GAAGATGCAATTCTGGAGGAGT Rev CGTAGCTTCTGGTCACATACAA
Acvr1c	For TCCCGAAATGCTTGATGATACA Rev TACTCCTCAACAACTCCTCCA
Taqman Assays from Life Technologies	**Cat#**
Zeb2	Mm00497193_m1
Cdh1	Mm00486918_m1
Tgfb1	Mm03024053_m1
Wnt5a	Mm00437347_m1
Tgfb1	Mm03024053_m1
Snail2	Mm00441531_m1
Tgfbr1	Mm00436964_m1
Primers for site-directed mutagenesis	**Sequence (5' to 3')**
SREBP1 Ala Forward	CTTGTCCCCTCCACCAGCGGCACCCGCTGC
SREBP1 Ala Reverse	GCAGCGGGTGCCGCTGGTGGAGGGGACAAG
SREBP1 Asp Forward	CTTGTCCCCTCCACCAGATGCACCCGCTGCTTTAAAG
SREBP1 Asp Reverse	CTTTAAAGCAGCGGGTGCATCTGGTGGAGGGGACAAG

Primers for chromatin immunoprecipitation (ChIP) and quantitative PCR
primers position is relative to transcription start site (+1)

Mouse *Tgfb1*		Forward	Reverse
-3204	-3032	TGTCAGTGCAGCTTTTCTGG	GCCACATTTGGAAACAGGTC
-2658	-2510	CTGGCCTTAGCTGTCTTCC	CAAAAAATGGTCCCGGAAAGAG
-2313	-2118	CACTGTGCTCTCAGGGTTG	AGGCTAGAACGGGGAGTC
-1934	-1778	GTGTGTGCCAAAATGTCACC	ACATTTGGGGCTGAACACT
-1506	-1293	CTCCAAGCATTGGACTGTCA	ACCTCCCTTTGTGGTCTCT
-1278	-1131	CTTGACTTGAGAGGTTGGACTT	TTGCCTGAATTTCCTCTCTGG
-831	-648	GCACGCAGATACCATCTACA	CTTCACTGCTGTGCCATTATG
-531	-357	TAGAAAGGGCTGTGGGTTG	GCAGACTTTGCGGATGAGA
-274	-97	GACCCTTCAACAACTCCCAA	GCACTGTCTTCATCTTAGCGT

+51	+176	CGCGGATCCTCCAGACA	TCCTCGGCTGCTCCTTT
+267	+375	GACGAGCTGGTTGAGAGAAG	CTGTCTGGAGTCCTCAGGT
+390	+564	GTGGACACTCGATCGCTAC	AGAGAGGGTCCTGGGATG
+717	+826	GCTTTCTCCCTCAACCTCAAA	CTCGGCAAAGGTGGGATG
Mouse *Ldlr*			
-38	+60	CGCTCAGTGAGGTGAAGATT	GCACGCCCAGAGTCATT
Sequences of guide RNA for CRISPRi targeting of mouse *Nsdhl*			
Position	Strand	Forward	Reverse
72918667	-	**CACC**GGCCGGTTGTCTGCAAGCTG	**AAAC**CAGCTTGCAGACAACCGGCC
72918711	+	**CACC**GCACACGCAGCAGCCTCTAA	**AAAC**TTAGAGGCTGCTGCGTGTGC
72918630	+	**CACC**GACCGGCAACCAGAGAAGTC	**AAAC**GACTTCTCTGGTTGCCGGTC